

Theiler's Murine Encephalomyelitis Virus Group Includes Two Distinct Genetic Subgroups That Differ Pathologically and Biologically

YAHLI LORCH,¹ ADAM FRIEDMANN,^{1*} HOWARD L. LIPTON,² AND MOSHE KOTLER³

Departments of Genetics¹ and Molecular Virology,³ Hebrew University of Jerusalem, Jerusalem, Israel, and Department of Neurology, Northwestern University, McGaw Medical Center, Chicago, Illinois 60611²

Received 19 March 1981/Accepted 30 June 1981

The intracellular development and RNA composition of Theiler's murine encephalomyelitis virus (TMEV) isolates were determined by electron microscopy, sucrose gradient centrifugation, and RNase T₁ fingerprinting. Replication of FA virus, a virulent strain of TMEV, was characterized by the appearance of viral crystalline arrays in the cytoplasm of infected cells. In contrast, cells infected with the less virulent isolates (WW, TO4, BeAn 8386, and Yale) showed no crystalline arrays; instead, virions were found to be arranged between two layers of membranes in the cytoplasm of infected cells. Analysis of the RNAs of TMEV isolates showed that the RNAs were single-stranded molecules having sedimentation coefficients of 35S. RNase T₁ fingerprinting of TMEV RNA revealed that striking differences between the virulent and less virulent TMEV isolates existed. Moreover, base composition analysis of RNase T₁-resistant oligonucleotides of two TMEV isolates which represented the two subgroups indicated that there were no substantial oligonucleotides common to both subgroups. Based on these findings and the known difference in virulence, we suggest that the TMEV group contains two genetically distinct subgroups of viruses.

Theiler's murine encephalomyelitis viruses (TMEV) are naturally occurring enteric pathogens of mice that belong to the Picornaviridae family (13, 16, 17). All TMEV share a close serological relationship; however, they can be divided into two subgroups based on their behavior *in vivo* and *in vitro* (9).

One subgroup includes two highly virulent viruses, GDVII and FA, which produce a fatal encephalitis in mice after intracerebral inoculation. The other subgroup includes DA, WW, TO4, BeAn 8386, and Yale viruses, which are far less virulent. After intracerebral inoculation with the less virulent isolates, mice develop persistent central nervous system infections. These persistent infections result in mononuclear cell infiltration of the leptomeninges and central nervous system white matter and in primary demyelination (3, 8). Recently, it was demonstrated ultrastructurally that the intracellular organization at late stages of infection of prototypes of the two TMEV subgroups differ markedly: GDVII virus formed crystalline arrays within the cell cytoplasm, and DA viruses did not form such crystals but instead were aligned between two membrane units (5).

In this study, we extended the ultrastructural studies to five additional TMEV isolates, and we

present data on the RNA compositions of all seven isolates. The electron microscopic study showed that the two TMEV subgroups differed in intracellular development. Analysis of TMEV RNA revealed that the sedimentation coefficient values of the viral RNAs of both subgroups were similar. However, the ribonuclease T₁ fingerprinting patterns of the two TMEV subgroups were markedly different.

Based on differences in pathogenesis (8), intracellular development, and oligonucleotide composition of the two subgroups, we suggest that the two subgroups of TMEV are genetically distinct groups of viruses.

MATERIALS AND METHODS

Cells. Baby hamster kidney cells (BHK-21) were maintained in Dulbecco modified Eagle medium containing 0.1 mM L-glutamine, 100 µg of streptomycin per ml, 100 U of penicillin per ml, 25 mM MgCl₂, and 10% fetal calf serum.

Viruses and virus assay. The GDVII, FA, DA, WW, TO4, BeAn 8386, and Yale isolates of TMEV were adapted for growth in tissue culture as previously described (8, 12). All viral isolates were plaque purified. Viruses were passed two or more times in cells at low multiplicities of infection to achieve higher virus titers. Virus titers were determined by standard plaque assay as previously described (11). The neurovirulence

of all strains was tested before their use in the experiments. It was confirmed that GDVII and FA isolates were highly virulent for mice and induced a rapidly fatal encephalitis after intracerebral inoculation. The DA, WW, TO4, BeAn 8386, and Yale virus isolates were less virulent and caused persistent demyelinating central nervous system infections in injected mice. Virus stocks used for testing the neurovirulence were later used for electron microscopic studies and RNA analyses. Neurovirulence and histopathology were determined as previously described (3, 12).

Radiolabeling of virus. Monolayers of BHK-21 cells in petri dishes (150 mm) were washed with warm, phosphate-free Dulbecco modified Eagle medium supplemented with 3% dialyzed calf serum and were incubated for 4 h at 37°C. After incubation, cultures were infected with 1 ml of virus at a multiplicity of infection of 10. [³²P]phosphate, carrier-free (Nuclear Research Center, Negev, Israel), was added to a final concentration of 0.5 mCi/ml. Cells were incubated at 37°C and observed for cytopathic effect. To label virus or cell RNA with [³H]uridine, we washed cultures with warm Dulbecco modified Eagle medium, and 10 μ Ci of [³H]uridine (19,300 mCi/mmol; Nuclear Research Center) per ml was added.

Virus purification. Virus was purified from infected cells by a modification of the procedure described by Ziola and Scraba (18). Lysates from infected monolayer cultures were disrupted by three cycles of freezing and thawing and were clarified at 10,000 $\times g$ at 4°C for 30 min in an RC2-B Sorvall centrifuge. Trypsin (Sigma Chemical Co. St. Louis, Mo.) was added to the supernatant (final enzyme concentration, 0.5 mg/ml), which was incubated at 37°C for 10 min, sodium dodecyl sulfate was added to give a final concentration of 1%, and the mixture was incubated at 24°C for 30 min. Virus was sedimented in a Beckman L5-50 ultracentrifuge at 85,000 $\times g$ at 24°C for 2 h in a Beckman type 35 rotor. Pellets were suspended in TNE buffer (10 mM Tris [pH 7.4], 100 mM NaCl, 1 mM EDTA) and sedimented through a discontinuous sucrose gradient (10 ml of 30% and 10 ml of 15%) at 24°C for 20 h at 100,000 $\times g$ in an SW27 rotor. The pellets were resuspended in TNE buffer, mixed with an aqueous solution of Cs₂SO₄ to give a final density of 1.33 g/ml, and centrifuged at 100,000 $\times g$ at 4°C for 24 h in an SW50.1 rotor. Viral bands were aspirated by puncturing the side of the tube with a syringe.

Preparation of viral RNA. RNA from purified virions was extracted and purified according to the method described by Kacian and Myers (7). The sedimentation coefficient of the viral RNA was determined in a 15 to 30% sucrose gradient in TNE buffer containing 0.5% sodium dodecyl sulfate. The gradient was centrifuged in an L5-50 Beckman ultracentrifuge equipped with an SW27 rotor at 100,000 $\times g$ for 16 h at 24°C. rRNA (18 and 28S) labeled with [³H]uridine was used as a size marker. Peaks of 35S were removed, and RNA was precipitated by the addition of two volumes of absolute ethanol at -20°C overnight. RNA was washed once with cold ethanol and stored in ethanol at -20°C until it was used.

Replicative form (RF) RNA was isolated from GDVII virus-infected cells 8 h postinfection when 50 to 60% of the cells were rounded. Isolation of RF RNA

was carried out according to Nomoto et al. (14), with the following modifications. DNase digestion was extended to 60 min at 37°C, the Sepharose 4B chromatography step was omitted and, instead, the double-stranded RNA was dialyzed against TEA buffer (0.1 M triethanolamine [Sigma Chemical Co.], 0.01 M EDTA [pH 8.3]) for 20 h at 4°C and then kept frozen.

Electron microscopy. (i) Electron microscopy of virus-infected cultures. Monolayers of BHK-21 cells grown in plastic flasks (75 cm³) were infected with TMEV isolates at a multiplicity of infection of approximately 50 as previously described (5). Infected cultures were harvested at 2-h intervals between 0 and 18 h postinfection, fixed in 1% isotonic glutaraldehyde, postfixed with osmium tetroxide in Millonig buffer (pH 7.2), dehydrated with ethanol, and embedded in epoxy resin (Epon 812). Thin sections were prepared and stained with uranyl acetate and lead citrate and were then examined in a Jeol 100CX electron microscope equipped with a side-entry goniometer.

(ii) Electron microscopy of RNA. Single-stranded viral RNA from 35S fractions was precipitated with ethanol, dried, and dissolved in TEA buffer. Ten microliters of RNA solution (1 to 3 μ g/ml) was mixed with 40 μ l of a solution containing 0.1 M TEA buffer, 5 M urea, and 80% formamide, pH 8.5. Ten microliters of cytochrome *c* solution (3 mg/ml) was added, and 50 μ l of the resulting substance was heated to 50°C for 3 min, cooled to 4°C, and spread on cold hypophase solution containing 1/100 TEA buffer. Freshly coated collodion grids were used to pick the RNA film. Grids were stained with uranyl acetate and rotary shadowed with platinum. GDVII virus RF RNA, isolated from virus-infected cells, was prepared for electron microscopy according to Jacobson and Spahr (6).

Fingerprinting of ³²P-labeled viral RNA. The two-dimensional electrophoresis technique for fingerprinting RNA was performed in accordance with the method of Billeter et al. (1, 2). The [³²P]RNA samples containing 100 μ g of yeast RNA in a small volume of water were lyophilized and digested with 8 μ l (16 U) of RNase T₁ (Sigma) in 20 mM Tris-hydrochloride (pH 7.5)-2 mM EDTA at 37°C for 30 min. The digested samples were mixed with xylene cyanol FF and bromophenol blue markers and applied to the first-dimension gel (200 by 400 by 2 mm), which consisted of 10% acrylamide, 6 M urea, and 0.025 M citric acid (pH 3.5). Electrophoresis was terminated when the xylene cyanol FF dye had migrated 20 cm from the origin. The second-dimension gel electrophoresis was terminated when the bromophenol blue dye reached the 18-cm mark. Autoradiography was performed with Afga-Gavaert Curix RP-2 film.

Fingerprinting analysis. In some experiments, oligonucleotides were further analyzed by elution from the second-dimensional gel and complete digestion with RNase A (1.5 μ g/50 μ g of RNA; Sigma), and the digestion products were separated by electrophoresis on Whatman DEAE paper at pH 3.5 as previously described (1, 2). Products were identified by their electrophoretic mobilities, and products containing three or more A residues were eluted from DEAE paper and subjected to complete digestion to nucleoside 2',3'-monophosphates with a mixture of RNases

A, T₁, and T₂ (1, 2). Yields of T₁ oligonucleotides were quantitated by counting Cerenkov radiation from gel pieces suspended in 0.3 ml of water containing 60 μ g of yeast RNA per ml, and pieces of DEAE paper containing the nuclease products were counted in toluene-based scintillation fluid.

RESULTS

Intracellular development of TMEV strains. We have previously shown that the intracytoplasmic development of GDVII virus differs from that of DA virus (5). Although well-

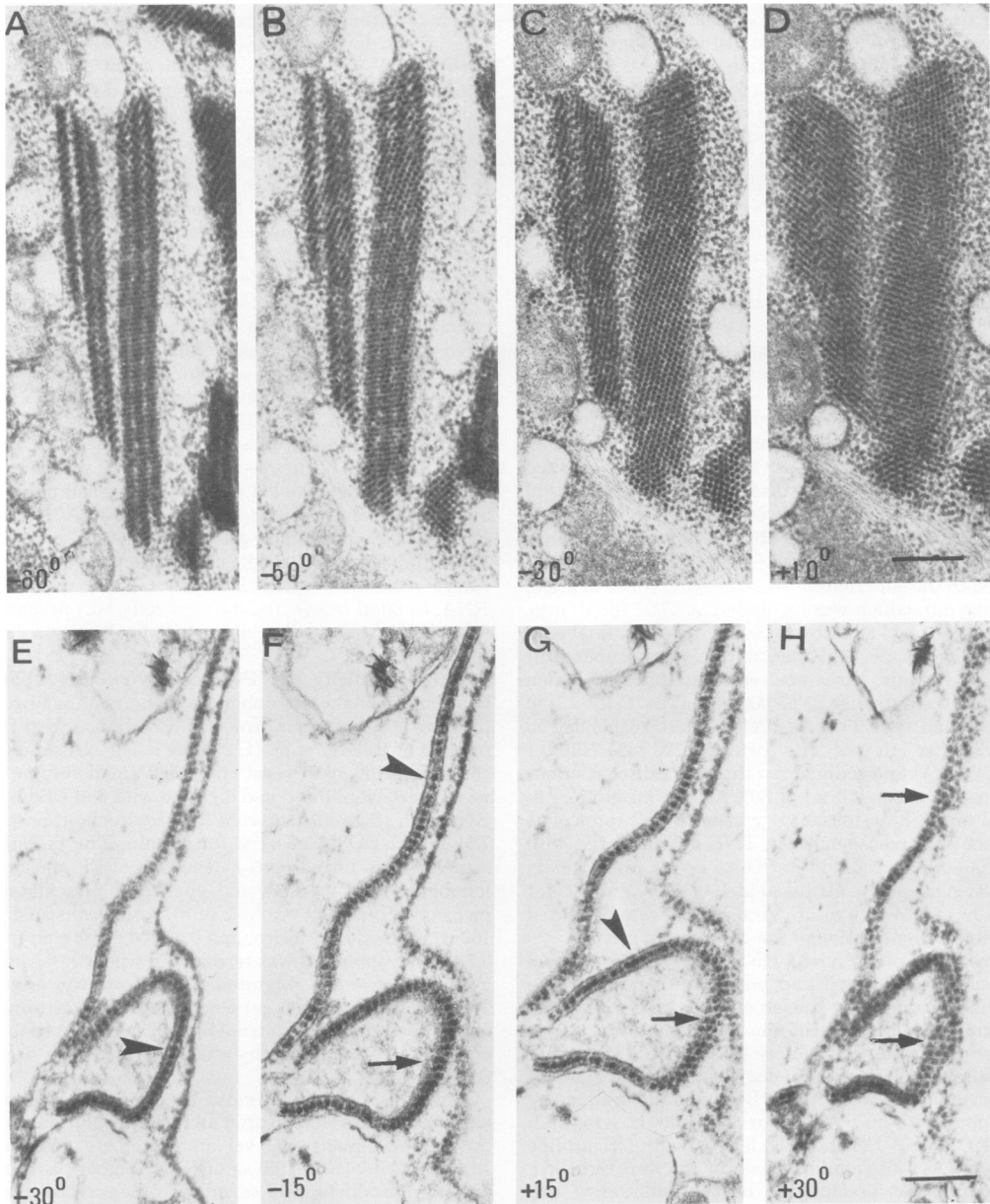


FIG. 1. (A through D) Series of electron micrographs of an FA virus-infected cell 7 h postinfection showing the complex structure of the viral crystal by the tilting of the crystalline array at different angles. Bar = 0.5 μ m. (E through H) Series of electron micrographs of a WW virus-infected cell 10 h postinfection. The micrographs display the tilting at different angles of viruses enclosed between the two membrane units. Heavy arrows point out areas where both membranes are evident; thin arrows point out similar areas when these areas were tilted. Bar = 0.2 μ m. The degrees of tilting are shown at the lower left sides of the pictures.

developed crystalline arrays of virions were observed in the cytoplasm of GDVII virus-infected cells, in DA virus-infected cells, virions were enclosed within two sheets of membranes. To find out whether the intracellular development of other TMEV isolates follows this pattern, the replication of five additional TMEVs in BHK-21 cells was examined by electron microscopy.

Cells infected with all isolates showed similar morphological changes in the early stages of infection (4 to 6 h). The nucleus became crescent shaped and was displaced to the periphery of the cell, the cytoplasm filled with foamy-like vesicles, and "viroplasm" bodies appeared (4). These changes were similar to those previously described for GDVII and DA viruses (5) and are typical for picornaviruses (4). However, the later stages of FA virus infection differed markedly from those of WW, TO4, BeAn, and Yale virus infections. FA virus formed large crystalline arrays of virions within the cytoplasm of infected cells; these arrays were similar to those formed by GDVII virus. Application of goniometer tilting to thin sections of viral crystalline arrays provided new information about their structures. Figure 1A through D presents the tilting at different angles of a thin section containing viral crystalline arrays. It can be seen that the

distances between the virions within the crystal depend on the tilting plane, indicating that the crystalline arrays of viruses have a complex, three-dimensional structure.

In contrast, the intracytoplasmic development of WW, TO4, BeAn, and Yale viruses resembled that of DA virus. Assembled virus particles were generally found to be arranged between two membranes in the infected cell cytoplasm. Goniometer tilting of thin sections containing these membranes provided evidence that the particles were arranged in a single file between two layers of membranes (Fig. 1E through H). When both membranes enclosing the virions were seen, only a single row of virions was observed (Fig. 1E and F). When the section was tilted, a cluster of virions was observed, and one or both membranes disappeared (Fig. 1F through H).

Sedimentation coefficient values and ultrastructures. All TMEV isolates contain RNA as their genetic material (Lorch and Friedmann, unpublished data). The sedimentation coefficient values and morphologies of the RNAs of representative isolates of the two TMEV subgroups were determined. RNAs from [³H]uridine- and ³²P-labeled GDVII and DA virus isolates were sized by sucrose velocity gradient centrifugation, using 18 and 28S ³²P-labeled

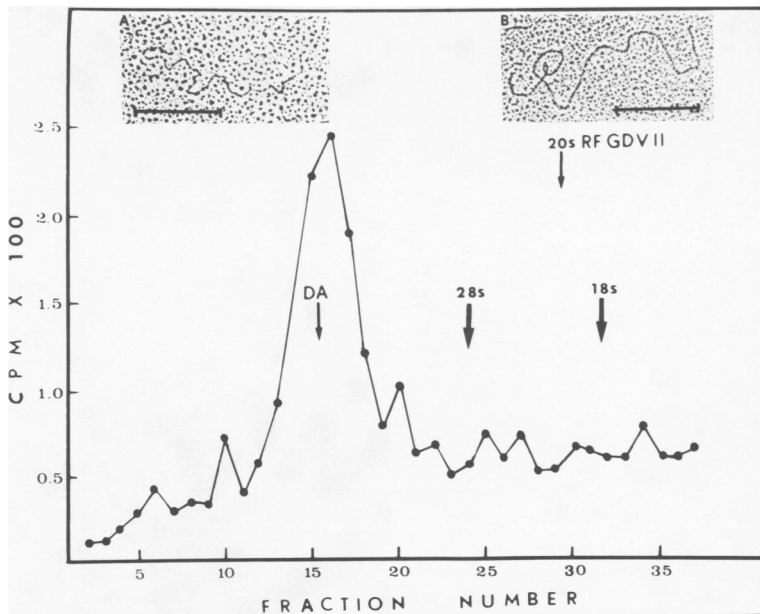
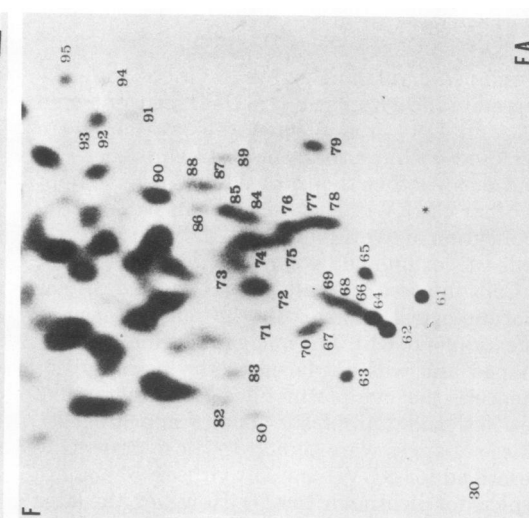
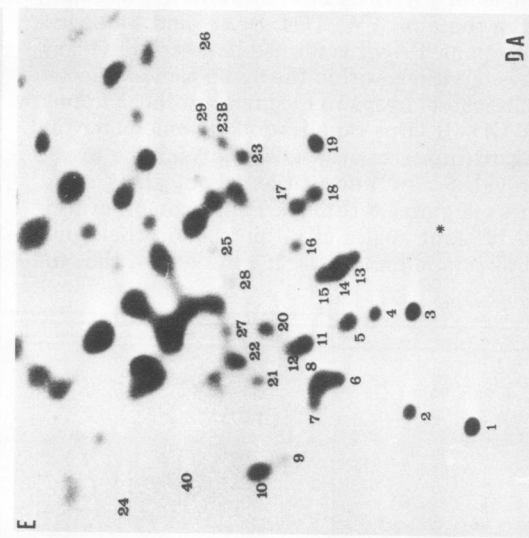
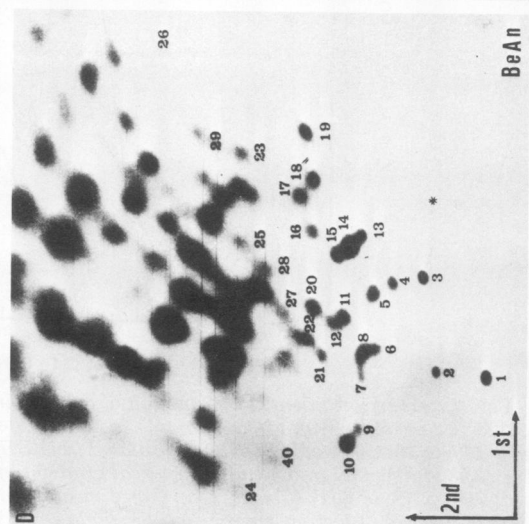
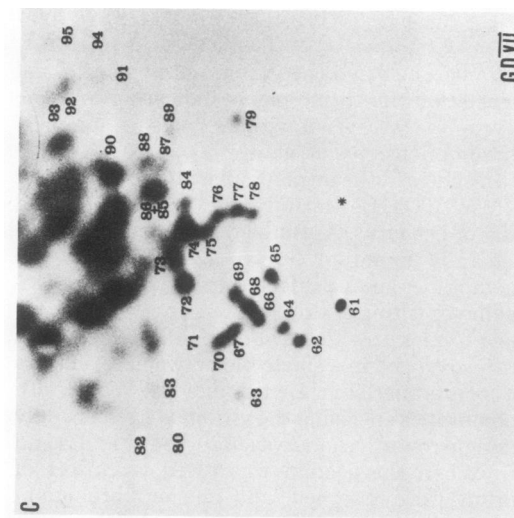
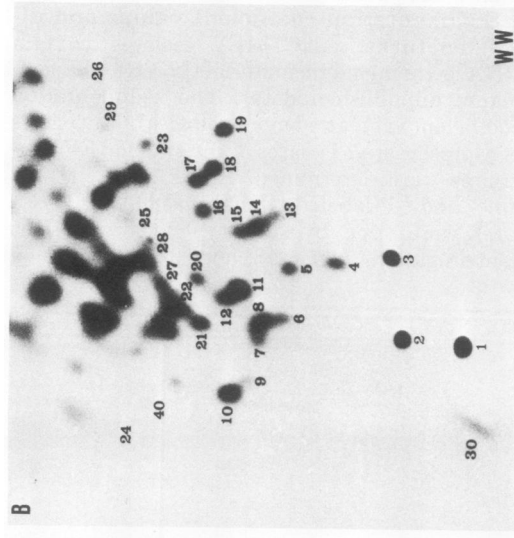
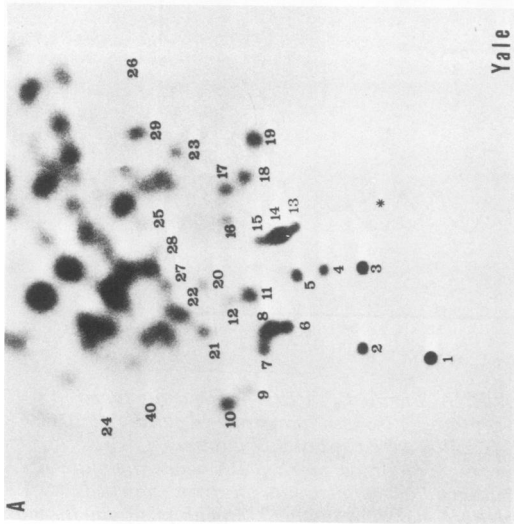


FIG. 2. Sucrose gradient centrifugation of GDVII virus RNA. Purified [³²P]RNA was centrifuged in a 15 to 30% (wt/wt) sucrose gradient prepared in TNE buffer containing 0.5% sodium dodecyl sulfate at 10,000 × g for 16 h at 20°C. 18 and 28S rRNAs (isolated from BHK-21 cells) were used as size markers. [³²P]RNA from DA virus sedimented in a parallel identical gradient appears as an arrow marked DA below the main RNA peak. RF RNA of GDVII virus, centrifuged in an identical gradient, appears as an arrow marked 20S RF GDVII. Inset A, Electron micrograph of single-stranded RNA banding at the 35S peak position. Inset B, Electron micrograph of GDVII virus RF RNA. (See text for details.) Bars = 0.5 μm.



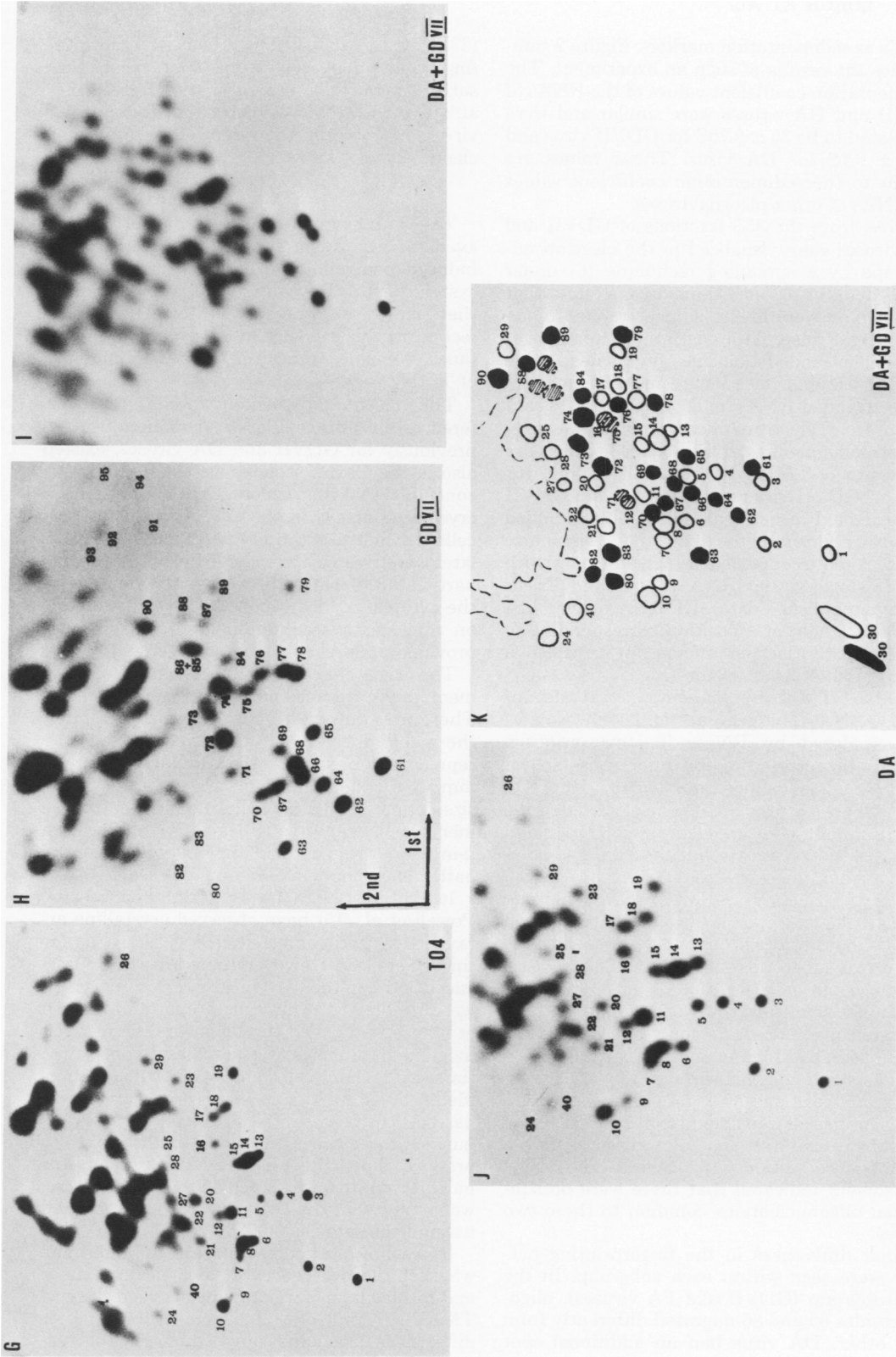


FIG. 3. Electrophoretic-chromatographic analysis (fingerprints) and autoradiography of RNase T₁-resistant, ³²P-labeled oligonucleotides of (A) Yale, (B) WW, (C) GDVII, (D) BeAn 8386, (E) DA, (F) FA, and (G) TO4 viruses. (H) through (K) represent coelectrophoresis of ³²P-labeled GDVII and DA-virus RNAs.

RNA's as sedimentation markers. Figure 2 summarizes the results of such an experiment. The sedimentation coefficient values of the RNAs of GDVII and DA viruses were similar and were calculated to be $35 \pm 0.75S$ for GDVII virus and $34.8 \pm 0.7S$ for DA virus. These values are similar to the sedimentation coefficient values for RNAs of other picornaviruses.

RNAs from the 35S fractions of GDVII and DA viruses were visualized in the electron microscope by a spreading technique (6) under strong denaturing conditions. It was found that these RNAs were linear, single-stranded molecules (Fig. 2, inset A). Length measurements of the single-stranded molecules gave a mean value of $2.2 \pm 0.6 \mu\text{m}$. Since length measurements of single-stranded RNA cannot be accurately estimated from electron micrographs because of intrastrand annealing, it was decided to measure the length of TMEV RF RNA. Therefore, RF RNA of GDVII virus was isolated from GDVII virus-infected cells. Isolated double-stranded RNA was sensitive to alkali and resistant to DNase, and it reannealed at high efficiency with GDVII single-strand RNA (Lorch and Friedmann, unpublished data). RF RNA banded in a sucrose gradient at a position corresponding to 20S (Fig. 2). Electron microscopy revealed a mean length of $2.6 \pm 0.3 \mu\text{m}$ (Fig. 2, inset B).

RNase T₁ fingerprinting analysis of TMEV RNA. The genomes of TMEV isolates were analyzed by RNase T₁ fingerprinting. Based on fingerprinting, the different isolates of TMEV can be divided into two distinct subgroups (Fig. 3A through G). The electrophoretic migrations of the oligonucleotides of GDVII and FA viruses were similar, but they differed completely from the patterns of DA, WW, TO4, BeAn, and Yale viruses, which resembled one another. To determine if the two subgroups had any oligonucleotides in common, representatives of the two subgroups, DA and GDVII viruses, were digested with RNase T₁ and electrophoresed individually and together. Among the well-separated oligonucleotides, only spot 75 partially overlapped spot 16, and spot 71 partially overlapped spot 12 (Fig. 3H through K).

The compositions of RNase T₁-resistant oligonucleotides of representative viruses of the two subgroups (WW and FA viruses) were determined by digestion with RNase A. The results (not shown) indicated that there were no substantial oligonucleotides common to these two viruses.

Minor differences in the fingerprinting patterns were seen within each subgroup. In the first subgroup (GDVII and FA viruses), oligonucleotides 85 and 86 migrated differently from each other. DA virus had an additional spot

(23B), which did not appear consistently in the fingerprint analysis. Several spots which had submolar ratios appeared in the fingerprints, although the RNA was extracted from purified virions. At present, the origin of these oligonucleotides is not known.

DISCUSSION

TMEV infection of mice is one of the few available experimental animal models of virus-induced demyelination of the central nervous system (9, 10). Revealing the TMEV functions that lead to the establishment of persistent infection in this model is of considerable importance. We have studied the basic characteristics of TMEV isolates.

The present study demonstrated that the differences in intracellular development, shown previously for GDVII and DA viruses, existed also in the TMEV isolates we tested. It can be concluded that the virulent TMEV isolates form crystalline arrays in the cytoplasm of infected cells. In contrast, the less virulent TMEV isolates were arranged as a single file of virions (one particle deep) between two membrane units in the cytoplasm. The use of the tilting technique on thin sections containing these membranes provided proof of this unique structure.

The origin, function, and composition of these membranes are not known at the present time. There are, however, at least two possibilities: the membranes are of cellular origin and may represent, for example, the endoplasmic reticulum, or the membranes may have been synthesized or modified as a result of infection. If these membrane structures appear *in vivo*, it will be tempting to suggest that they play a role in the pathogenesis of demyelinating disease.

It is interesting that in contrast to our results, Powell et al. (15) have observed crystalline arrays in DA virus-infected cells. The reason for this is not clear. However, there are a few differences between the two stocks of DA virus which we can point out: the virus preparation Powell et al. used produced the biphasic disease when inoculated into mice, was then passed only three times in BHK-21 cells, and was not plaque purified. In contrast, our virus preparation was passed many times in BHK-21 cells, was plaque purified three times, and had lost the ability to produce the acute phase by the time it was inoculated into mice. Based on these differences, we assume that the DA virus Powell et al. used was not the same as our DA virus.

It was of particular interest to determine whether the differences in biological behavior and intracellular development between the two TMEV subgroups resulted from minor or major differences in genome composition. For this rea-

son, the RNAs of seven TMEV were analyzed. We found that the sedimentation coefficients of all TMEV had similar values of approximately 35S. RNAs from representative virus isolates, studied by electron microscopy, proved to be single stranded molecules. In addition, RF RNA isolated from GDVII virus-infected cells had a mean length of $2.6 \pm 0.3 \mu\text{m}$. Based on the sedimentation coefficient value of virion RNAs and the lengths of 35S single-stranded and RF RNAs, it was possible to estimate the molecular size of TMEV RNA as 2.6×10^6 to 2.9×10^6 daltons.

The RNase T₁-resistant oligonucleotide fingerprint analyses of seven TMEV showed that the fingerprints of FA and GDVII virus isolates were similar but differed from those of DA, WW, TO4, BeAn 8386, and Yale viruses. Thus, the virulent and less virulent subgroups of TMEV differed in their fingerprint patterns. It is interesting that although the viruses of the TMEV group were isolated independently and at different places, the RNA fingerprints of each subgroup were similar or identical. An additional analysis of the base composition of oligonucleotides eluted from the two-dimensional gels of WW and FA virus RNAs revealed that all the substantial oligonucleotides of these two isolates were different. Furthermore, coelectrophoresis of GDVII virus and DA virus RNase T₁-resistant oligonucleotides showed that the oligonucleotides of these viruses had different electrophoretic mobilities. Taken together, these findings indicate that although the well-separated oligonucleotides of the RNA fingerprints represent some 10 to 15% of the total RNA genome, the two TMEV subgroups represent two different genomes.

Based on the differences in virulence (10-12), intracellular development, and RNA composition, we concluded that the TMEV group contains two genetically distinct virus subgroups.

LITERATURE CITED

1. Billeter, M. A., J. T. Parsons, and J. M. Coffin. 1974. The nucleotide sequence complexity of avian sarcoma virus RNA. *Proc. Natl. Acad. Sci. U.S.A.* 71:3560-3564.
2. Coffin, J. M., and M. A. Billeter. 1976. A physical map of the Rous sarcoma virus. *J. Mol. Biol.* 100:293-318.
3. Dal Canto, M. C., and H. L. Lipton. 1979. Recurrent demyelination in chronic central nervous system infection produced by Theiler's murine encephalomyelitis virus. *J. Neurol. Sci.* 42:391-405.
4. Dales, S., H. J. Eggers, I. Tam, and G. E. Palade. 1965. Electron microscope study of the formation of poliovirus. *Virology* 26:379-389.
5. Friedmann, A., and H. L. Lipton. 1980. Replication of Theiler's murine encephalomyelitis viruses in BHK21 cells: an electron microscopic study. *Virology* 101:389-398.
6. Jacobson, A. B., and P. F. Spahr. 1977. Studies on the secondary structure of single-stranded RNA from the bacteriophage MS2. II. Analysis of the RNase IV cleavage products. *J. Mol. Biol.* 115:279-294.
7. Kacian, D. L., and J. C. Myers. 1976. Synthesis of extensive, possibly complete, DNA copies of poliovirus RNA in high yields and at high specific activities. *Proc. Natl. Acad. Sci. U.S.A.* 73:2191-2195.
8. Lipton, H. L. 1975. Theiler's virus infection in mice: an unusual biphasic disease process leading to demyelination. *Infect. Immun.* 11:1147-1155.
9. Lipton, H. L. 1978. The relationship of Theiler's mouse encephalomyelitis virus plaque size with persistent infection, p. 679-689. *In* J. Stevens, G. J. Todaro, and C. F. Fox (ed.), *Persistent viruses: ICN-UCLA Symposia on Molecular and Cellular Biology*, vol. 22. Academic Press, Inc., New York.
10. Lipton, H. L. 1978. Characteristics of TO strains of Theiler's mouse encephalomyelitis viruses. *Infect. Immun.* 20:869-872.
11. Lipton, H. L. 1980. Persistent Theiler's murine encephalomyelitis virus infection in mice depends on plaque size. *J. Gen. Virol.* 47:169-177.
12. Lipton, H. L., M. C. Dal-Canto, and S. G. Rabinowitz. 1977. Chronic Theiler's virus infection in mice, p. 505-508. *In* D. Schlessinger (ed.), *Microbiology—1977*. American Society for Microbiology, Washington, D.C.
13. Lipton, H. L., and A. Friedmann. 1980. Purification of Theiler's murine encephalomyelitis virus and analysis of the structural virion polypeptides: correlation of the polypeptide profile with virulence. *J. Virol.* 33:1165-1172.
14. Nomoto, A., A. Jacobson, Y. Fon Lee, J. Dunn, and E. Wimmer. 1979. Defective interfering particles of poliovirus: mapping of the deletion and evidence that the deletion in the genomes of DI (1) and (3) are located in the same region. *J. Mol. Biol.* 128:179-196.
15. Powell, H. C., J. R. Lehrich, and B. G. Arnason. 1977. Electron-microscopic appearance of the DA virus, a demyelinating murine virus. *J. Neurol. Sci.* 34:15-23.
16. Theiler, M. 1937. Spontaneous encephalitis of mice, a new virus disease. *J. Exp. Med.* 65:705-719.
17. Theiler, M., and S. Gard. 1940. Encephalomyelitis of mice: epidemiology. *J. Exp. Med.* 79:79-90.
18. Ziola, B., and D. G. Scraba. 1974. Structure of the mengo virion. I. polypeptide and ribonucleate components of the virus particles. *Virology* 57:531-542.